



ELSEVIER

Contents lists available at ScienceDirect

## Chemical Engineering Journal

journal homepage: [www.elsevier.com/locate/cej](http://www.elsevier.com/locate/cej)Chemical  
Engineering  
Journal

## Kinetic modelling of the solventless synthesis of solketal with a sulphonic ion exchange resin

Jesús Esteban, Miguel Ladero\*, Félix García-Ochoa

Department of Chemical Engineering, College of Chemical Sciences, Complutense University of Madrid, 28040 Madrid, Spain

## HIGHLIGHTS

- Solketal synthesis with the sulphonic ion exchange resin Lewatit GF101 was studied.
- External and internal mass transfer limitations were evaluated.
- The effect of temperature, catalyst load and molar excess of acetone were assessed in kinetic runs.
- Several pseudo-homogeneous, ER and LHHW-based kinetic models were proposed.
- Physical and statistical discrimination advocates for an ER model.

## ARTICLE INFO

## Article history:

Received 13 October 2014

Received in revised form 19 January 2015

Accepted 27 January 2015

Available online 4 February 2015

## Keywords:

Solketal

Glycerol

Solventless synthesis

Kinetic model

Ion exchange resin

## ABSTRACT

Synthesis of solketal from acetone and glycerol is approached in this work through a batch process in the absence of solvents. A heterogeneous catalysis approach was employed using the resin Lewatit GF101 as catalyst after selection from a few other sulphonic ion exchange resins. An initial study of the external mass transfer revealed that a stirring rate of 750 rpm sufficed for the external mass transfer not to be the rate limiting step. Similarly, a study of the internal mass transfer showed that for particle sizes of 190  $\mu\text{m}$  the maximum reaction rate was achieved. Once the optimal stirring and particle size conditions were determined, a series of kinetic runs was conducted varying temperature (30–40 °C), initial molar excess of acetone to glycerol (3–12) and catalyst load (0.5–1% w/w) for this reaction in equilibrium. Different kinetic models based on potential laws and Eley–Rideal (ER) and Langmuir–Hinshelwood–Hougen–Watson (LHHW) equations were proposed to fit to the experimental data obtained. After physical and statistical discrimination, an ER accounting for the direct and reverse reaction was selected, with activation energies of  $124.0 \pm 12.9 \text{ kJ mol}^{-1}$  and  $127.3 \pm 12.6 \text{ kJ mol}^{-1}$  for the direct and reverse reaction, respectively, and enthalpy of adsorption of  $128.0 \pm 21.4 \text{ kJ mol}^{-1}$  for the adsorption constant of water.

© 2015 Elsevier B.V. All rights reserved.

## 1. Introduction

Despite glycerol (Gly) having been widely employed throughout history in multiple applications, the overproduction caused by the blooming biodiesel industry has caused a drop of its price. It is foreseen that environmental policies in the European Union will continue to spur the development of renewable sources of energy in the following years as stated in the EU 2009/28/EC Directive. As a consequence of such availability, glycerol has been widely regarded as a platform chemical from which assorted reactions can be proposed to yield valuable products. Due to its rich chemical reactivity, assorted valuable compounds through chemical routes of very distinct nature have been obtained [1–6].

Among the uses of products derived from glycerol, the utilisation of oxygenate derivatives as biofuel additives is receiving increasing attention. One example would be di and tritert-butyl glycerol (DTBG and TTBG) [7,8], which have proven to enhance the octane index of gasoline [9] as well as decrease viscosity of biodiesel, thus improving its cold-flow properties [10] while also reducing emissions of particulates, CO and certain aldehydes [11].

Ketals derived from the acetalisation of glycerol, have been more profusely studied as additives to fuels [8,12–15]. 1,2-isopropylidenglycerol, also referred to as solketal (Sk), has received particularly high attention, for it has proven to enhance certain performance parameters and specifications. Reduced gum formation and improvement of the octane index was observed when using up to 5% volume of solketal to gasoline [16], while addition of said ketal to biodiesel not only improved its viscosity, but also complied with the flash point and oxidation stability specifications

\* Corresponding author. Tel.: +34 913944164; fax: +34 913944179.

E-mail address: [mladero@quim.ucm.es](mailto:mladero@quim.ucm.es) (M. Ladero).

**List of abbreviations***Components*

Ac	acetone
Gly	glycerol
Sk	solketal
W	water

*Nomenclature*

<sup>1</sup> H-NMR	proton nuclear magnetic resonance
A, B and C	fitting parameters of the Hoerl curve (Eq. (1))
AIC	Akaike's information criterion
C	concentration of the components at a given time (mol L <sup>-1</sup> )
E <sub>ai</sub> /R	Ratio of activation energy and the ideal gas constant (K)
ER	Eley–Rideal kinetic model
F	Fischer's F statistical parameter
ΔH <sub>aw</sub> /R	ratio of the heat of adsorption of water and the ideal gas constant (K)
k	kinetic constants of the direct and reverse reaction
K	adsorption constant in the ER and LHHW models
LHHW	Langmuir–Hinshelwood–Hougen–Watson kinetic model
M	initial molar ratio of acetone to glycerol
n	total number of components
N	total number of data to which a model is fitted
P	number of parameters of the proposed model or potential model
PL	kinetic model based on potential laws, i.e., pseudohomogeneous

R	ideal gas constant (J mol <sup>-1</sup> K <sup>-1</sup> )
r	reaction rate (mol L min <sup>-1</sup> )
RMSE	residual mean squared error
t	time (min)
T	temperature (°C or K)
VE	variation explained (%)
Y	yield to product

*Greek letters*

η	effectiveness factor (defined by Eq. (2))
ν	stoichiometric coefficient of the component <i>i</i>
ω	agitation rate (rpm)

*Subscripts*

0	relative to the start of the reaction, time equals zero
<i>i</i>	relative to component <i>i</i>
cat	relative to the catalyst
max	relative to the maximum rate of reaction observed using different particle sizes
w	relative to water in the adsorption constant

*Superscripts*

130	relative to the rate of reaction observed when a particle size of 130 μm was used
d <sub>p</sub>	relative to the rate of reaction observed using a particle size of d <sub>p</sub>

as enacted by European and American Standards (EN 14214 and ASTM D6751, respectively) [17]. Even further reactions of solketal have been explored to yield new potential additives, namely: its upgrade to benzyl alcohol ether [18] or the synthesis of solketal *o*-methylesters by making solketal react with dialkyl carbonates under basic conditions [19].

In addition to the mentioned applications enhancing the performance parameters of certain fuels, solketal has been put to use as a plasticizer and a green solvent and suspending agent in pharmaceutical formulations [20]. Furthermore, its chemical reactivity makes it a relevant building block in the synthesis of chemicals of pharmaceutical interest like prostaglandins, glycerophospholipids or β-blockers like (*S*)-propranolol, widely used for medical treatments like hypertension or migraine [21,22].

The synthesis of acetals mainly consists in the reaction of an alcohol with ketones or aldehydes. Specifically, cyclic ketals (like solketal) may be obtained through the reaction of polyols (like glycerol) with said carbonyl compounds through a reaction mechanism that consists of the formation of a highly unstable intermediate species and then the cyclation of said intermediate to yield the ketal [23,24].

Assorted catalysts have been employed to such purpose. Approaches to completion of this reaction using homogeneous catalysis have been made, such as employing *p*-toluenesulphonic, sulphuric or hydrochloric acids [17,25–27]. Efforts using solid catalysts appear to be the most followed trend, including the use of oxides of Group IV of the periodic table [28], zeolites [29,30], clays [29], heteropolyacids immobilized in silica [31], sulphonic acid-functionalized mesostructured silicas [32,33], promoted zirconia [34], various sulphonated carbon silica mesocomposite materials [35], Sn-based salts, mesoporous substituted silicates [33]. With respect to the utilisation of solid catalysts, special mention must be made to the use of commercially available ion exchange resins. Table 1 compiles a brief review of the references found using such

catalysts together with the conditions and operation modes used in each work to shift the equilibrium existing in this reaction towards the products [29,30,36–39]. Selectivity of these catalysts towards the five-membered ring isomer of solketal has been reported to be practically 100% for the vast majority of the aforementioned acid catalysts.

Operational aspects of the reaction of glycerol with acetone (Ac) to yield solketal include a wide array of temperatures from room temperature or slightly above [34] to temperatures exceeding the acetone boiling point (57 °C), in which case removal of water is sought in order to shift the equilibrium to the products through a reactive distillation process [17,31,40]. Use of supercritical conditions at 250 °C and 8 MPa has also been reported in literature, with conversions of glycerol being no greater than 29%; the absence of catalyst is ascribed to the catalytic effect of the acidic strength of the alpha hydrogen of acetone in the gas phase [41].

Moreover, molar excess of acetone with respect to glycerol (*M*) has also been used in order to shift the reaction to the products given the existing equilibrium. Typical *M* values mentioned in literature range from 2/1 to 6/1, despite sometimes being as high as 10.8/1 [41] or even 20/1 in order to reach yields of 82% of solketal under reflux conditions [42]. More recently, excess of acetone was used together with ethanol acting as a cosolvent [36,37,43] for acetone and glycerol, considering the limited miscibility of these compounds at the start of the reaction [44].

Reaction kinetics is an essential tool to deepen the understanding of chemical processes. Kinetic models concerning reactions implied in the valorisation of glycerol have been found [8,45–47] and even a kinetic model for the synthesis of solketal has recently been reported for a procedure using ethanol as a cosolvent over Amberlyst 35 [36].

The aim of this work is to describe the catalytic ketalization of glycerol with acetone under solventless conditions with sulphonic ion exchange resins. For this purpose, screening among some

**Table 1**  
References found in literature using sulphonic ion exchange resins in the synthesis of solketal.

Refs.	Ion exchange resin	T (°C)	M	Catalyst load	Other details <sup>a</sup>	Y <sub>Sk</sub> (%)
[29]	Amberlyst 36	40	2.7:1.8:1 <sup>b</sup>	1.2% w/w	Operation with water removal using dichloromethane as solvent	88
[30]	Amberlyst DPT-1	70	3	5% w/w	Counter-current reaction distillation column	98
[36]	Amberlyst 35	50	1:2:1 <sup>b</sup>	2% w/w	Batch operation using methanol as solvent	65
[37]	Amberlyst 35 and Amberlyst 36	40	1:6:1 <sup>b</sup>	–	Operation in fixed bed using methanol as solvent. P = 4,14 MPa, WHSV <sup>c</sup> =4 h <sup>-1</sup>	88
[38]	Amberlyst 15	70	1.2	15% mol	Water removal by unknown method to shift equilibrium <sup>d</sup>	95
[39]	Amberlyst 15	70	2	3.18% w/w	Water removal by unknown method to shift equilibrium <sup>d</sup>	95

<sup>a</sup> At atmospheric pressure unless otherwise specified.

<sup>b</sup> Molar ratio solvent:acetone:glycerol.

<sup>c</sup> WHSV: weight hourly space velocity.

<sup>d</sup> Operation mode not explicitly stated in the reference, though it can be inferred from the yield achieved with such a low molar excess of acetone.

resins as well as a study of the operating conditions to avoid internal and external mass transfer resistance is made. Most importantly, the effect of operating variables is evaluated and suggestion and physicochemical and statistical discrimination among different kinetic models is made to propose a reaction mechanism.

## 2. Materials and methods

### 2.1. Materials

Extra pure glycerol (99%) (Scharlau Chemie, Ltd.) and acetone (HPLC grade) (Romil, Ltd.) were utilised as reactants. Solketal (purity = 98.1%) from Aldrich was employed for calibration purposes. Finally, the preparation of samples required methanol (HPLC grade) (Fisher Scientific UK, Ltd.) as internal standard and deuterium oxide (99.8%, NMR spectroscopy grade) (Scharlau Chemie, Ltd.) as solvent. The sulphonic ion exchange resins utilised were: Purolite CT275DR, Purolite CT276 (Purolite, Ltd.); Amberlyst 35dry, Amberlyst 36dry (Rom and Haas France SAS) and Lewatit GF101 (Lanxess Deutschland GmbH). All of them were kindly supplied by each manufacturer.

### 2.2. Experimental

#### 2.2.1. Apparatus, methodology

The reactor employed to perform the ketalization runs is schematized in Fig. 1. It consists of a glass vessel whose outer walls are heated by a thermal controlled by an OMRON E5CN PID controller

with temperature being measured with a thermocouple. The loads were stirred by means of a flat six-blade impeller whose speed was regulated by an IKA RW20 motor (250–2500 rpm). Finally, sample withdrawal was performed thanks to a syringe with a wide-bore needle piercing a Teflon lid tightly fitted to the top of the reactor.

The operational procedure started by loading the appropriate amount of both reactants into the glass reactor. Then, stirring and heating were initiated and, once the temperature reached its set value, catalyst was added through the inlet too and reaction started to take place. Prior to conducting the reactions, resin beads were crushed and sieved when necessary.

#### 2.2.2. Analysis

Samples were analysed by <sup>1</sup>H NMR spectroscopy with a BRUKER DPX 300 MHz BACS60 device. Deuterium oxide was employed as solvent for the samples and methanol as an internal standard. Solketal was the chemical species followed, with a signal of representative protons of this chemical being identified and used for quantification. This signal corresponds to chemical shifts of 1.27 and 1.33 ppm.

### 2.3. Mathematical methods

The data obtained from the kinetic runs were regressed following distinct kinetic models. For this purpose Aspen Custom Modeler was used, in which fitting is conducted applying the Levenberg–Marquardt algorithm together with the numerical integration of each proposed model through a fourth-order Runge–Kutta method. First, the models were individually fitted to experimental data at fixed temperature values; then, multivariable fitting of the experimental data available was completed, including temperature.

The kinetic models herein proposed have been selected on a physicochemical basis, while discrimination and final selection among them has been made following both physicochemical and statistical criteria. Among the latter, the next have been regarded: Fischer's *F* value (*F*), residual mean squared error (*RMSE*), variation explained (*VE*) [48] and Akaike information criterion (*AIC*) [49]. These statistical parameters and criteria are defined in detail elsewhere [50] and in the Supplementary material. They have previously been used successfully for kinetic modelling discrimination purposes [51]. In statistical terms, the adequacy and quality of the proposed models to describe the observed data improves as the value of *F* and *VE* increase and as *AIC* and *RMSE* decrease.

## 3. Results and discussion

### 3.1. Selection of a sulphonic ion exchange resin

As appointed in Section 1, some sulphonic resins have been studied in acetalisation reactions. For this reason, we tested the

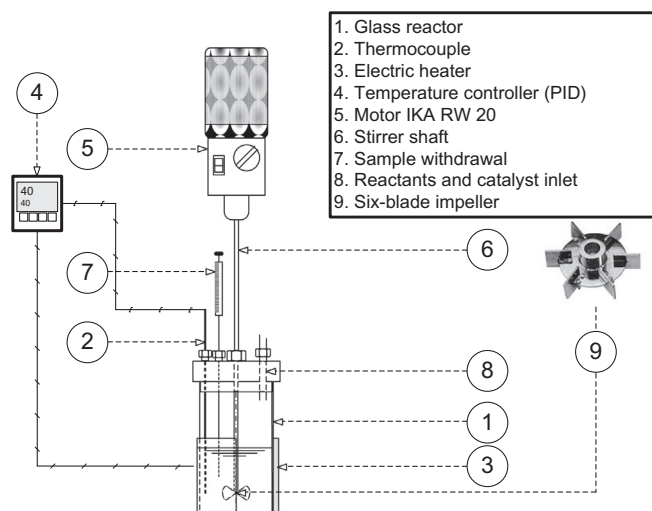


**Fig. 1.** Experimental setup for the synthesis of solketal from glycerol and acetone.

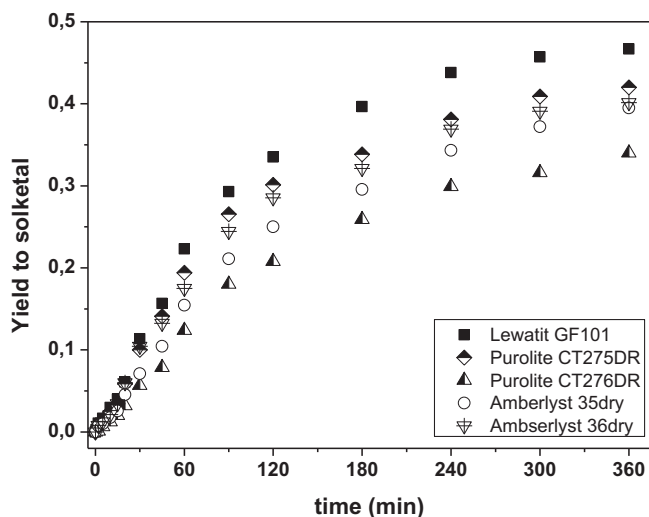


**Fig. 2.** Comparison of the yield to product achieved among five different sulphonic ion exchange resins. Conditions:  $T = 40\text{ }^{\circ}\text{C}$ ,  $M = 4.5$ , catalyst load = 0.5% w/v and  $\omega = 750\text{ rpm}$ .

**Table 2**

Properties of the ion exchange resin Lewatit GF101, used for the synthesis of solketal.

Appearance	Beige opaque solid	Pore volume <sup>d</sup> ( $\text{cm}^3\text{ g}^{-1}$ )	0.270
Maximum operating temperature <sup>a</sup> (K)	403	Surface area <sup>d</sup> ( $\text{m}^2\text{ g}^{-1}$ )	48
Acid capacity <sup>b</sup> ( $\text{eq H}^+\text{ kg}^{-1}$ )	5.11	Bulk density <sup>d</sup> ( $\text{g cm}^{-3}$ )	1.15
BET surface area <sup>c</sup> ( $\text{m}^2\text{ g}^{-1}$ )	28	Apparent density <sup>d</sup> ( $\text{g cm}^{-3}$ )	1.67

<sup>a</sup> From supplier.

<sup>b</sup> Obtained from ion exchange with NaCl.

<sup>c</sup> Obtained from BET.

<sup>d</sup> From mercury porosimetry.

resins Lewatit GF101, Purolite CT275DR and CT276 for performance in addition to Amberlyst 35dry and 36dry. Fig. 2 shows the evolution of the yield to product using the mentioned resins, in which it can be observed that Lewatit GF101 achieves the best results. Table 2 compiles some basic features of this resin, which has been selected as the catalyst for subsequent experimental work.

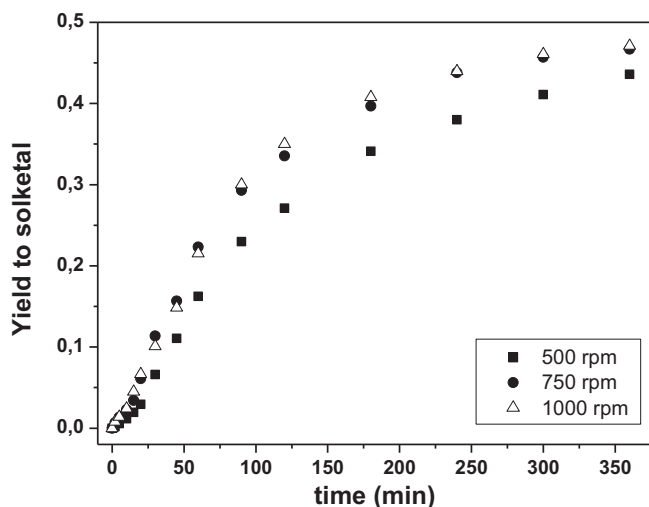


**Fig. 3.** Effect of the agitation speed on the evolution of the reaction. Conditions:  $T = 40\text{ }^{\circ}\text{C}$ ,  $M = 4.5$ , catalyst load = 0.5% w/v.

### 3.2. Effect of external mass transfer

External mass transfer could play a primary role limiting the overall rate of reaction in heterogeneously catalysed systems. In the case studied in this work, this effect can be even higher considering that acetone and glycerol have limited miscibility prior to the generation of the reaction products [44]. The performance of the reaction was evaluated at different stirring speeds were assessed at  $40\text{ }^{\circ}\text{C}$ , the highest temperature of the range. Fig. 3 demonstrates no perceivable difference in the evolution of the yield to product using stirrer speeds above 750 rpm. For this reason, this value was selected to perform further experimentation without the limitation of external mass transfer. Despite the fact that a solventless system was used in this case contrary to the utilisation of ethanol as solvent in a previous work, the mentioned stirrer speed value agrees well with that reported in such work, in which 700 rpm was used [36]. In turn, this means that the presence of two liquid phases and the high difference in viscosity between acetone ( $0.21\text{ cP}$  at  $40\text{ }^{\circ}\text{C}$  [52]) and glycerol ( $284\text{ cP}$  at  $40\text{ }^{\circ}\text{C}$  [53]) do not have an effect on external mass transfer compared to a single phase liquid system aided by the presence of a cosolvent species.

### 3.3. Effect of internal mass transfer

In order to assess the effect of internal mass transfer for this reaction using Lewatit GF101, the ketalization reaction was completed employing different particle sizes. Fig. 4 shows the particle size obtained by sieving the catalyst as received from the supplier. Though the particle size ranges were not equal in all cases represented in the figure, it can be seen that resin beads between 500 and  $800\text{ }\mu\text{m}$  represent slightly over 50% of the total amount of particles.

An assessment of the internal mass transfer is displayed in Fig. 5a, in which several particle sizes of Lewatit GF101 were evaluated for activity. A comparison is made using the catalyst as supplied (i.e. non-sieved), different fractions of the sieved catalyst in the range  $200 < d_p < 1000\text{ }\mu\text{m}$  and grinded particles below  $200\text{ }\mu\text{m}$ , owing their absence in the resin as received. Additionally, to test whether grinding could potentially have an effect on the activity of the resins, Fig. 5b bears witness of the evolution of the yield to solketal using two particular fractions of the resin after crushing and sieving comparing it with that of the sieved particles with no treatment. It can be observed that the difference between

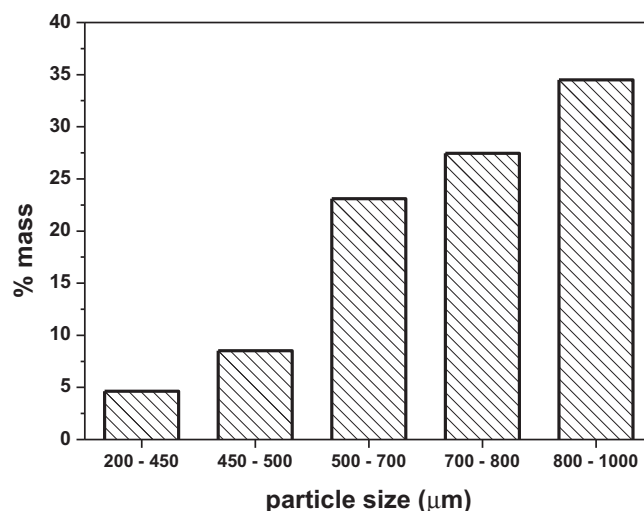


**Fig. 4.** Particle size distribution of Lewatit GF101 obtained by sieving.

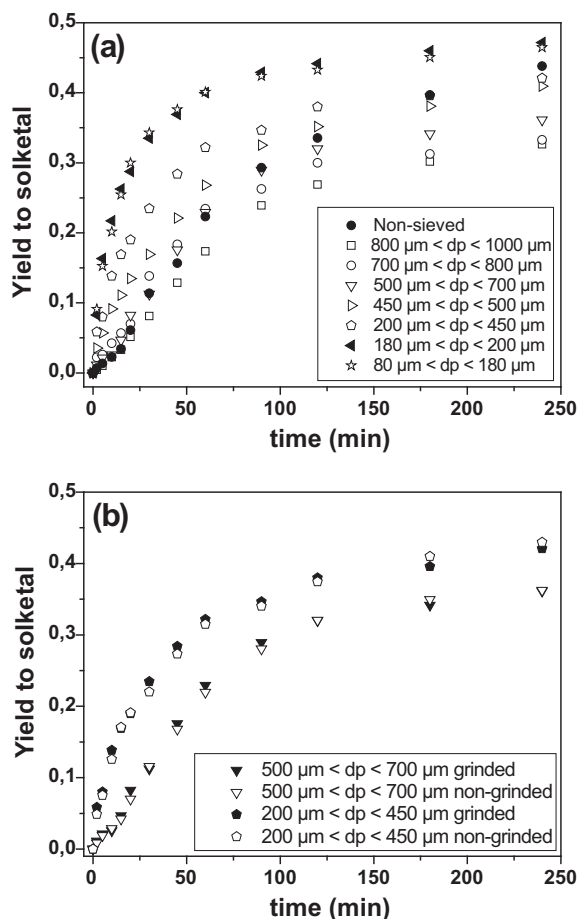


Fig. 5. Comparison of the evolution of the yield to solketal using non-sieved and sieved particles of Lewatit GF101 at selected particle sizes (a) and assessment of the effect of grinding and not grinding resin beads at selected particle sizes (b). Conditions:  $T = 40\text{ }^{\circ}\text{C}$ ,  $M = 4.5$ , catalyst load = 0.5% w/v,  $\omega = 750\text{ rpm}$ .

using the resin with or without crushing is not remarkable. This fact had already been observed.

A Hoerl curve was fitted to the observed data of the concentration of solketal with respect to time. The maximum reaction rates for each assay at a different particle size were obtained from the differentiation of the mentioned curve, whose equation is defined as follows [54]:

$$C_{\text{Sk}} = A \cdot B^t \cdot t^C \quad (1)$$

in which  $C_{\text{Sk}}$  is the concentration of solketal ( $\text{mol L}^{-1}$ ),  $t$  is time and  $A$ ,  $B$  and  $C$  are the fitting parameters of the equation. Fig. 6 depicts the effectiveness factor, defined by Eq. (2):

$$\eta = \frac{r_{\text{max}}^{d_p}}{r_{\text{max}}^{130}} \quad (2)$$

where  $r_{\text{max}}^{d_p}$  stands for the maximum rate observed at each particle size and  $r_{\text{max}}^{130}$  corresponds to the maximum rate of solketal production observed at 130 μm (average value of the interval  $80 < d_p < 200\text{ }\mu\text{m}$ ), diameter at which negligible internal diffusion effects can be considered to be present. Thus, from Fig. 6 can be inferred that a particle size between 180 μm and 200 μm can be used without internal mass transfer limitations.

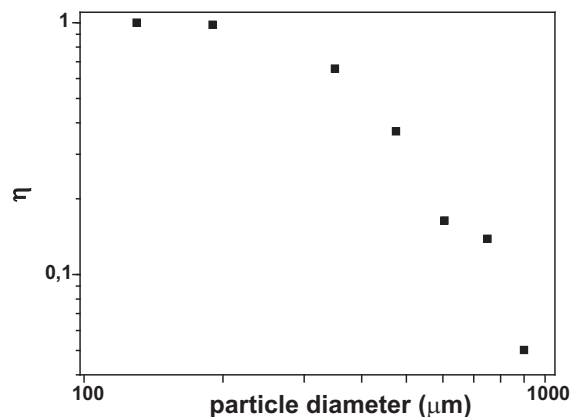


Fig. 6. Influence of the particle size on the maximum reaction rates observed at each particle size. Conditions:  $T = 40\text{ }^{\circ}\text{C}$ ,  $M = 4.5$ , catalyst load = 0.5% w/v.

### 3.4. Effect of temperature, catalyst load and initial molar ratio of reactants

With the stirring rate and particle size fixed at values at which no external and internal mass transfer limitations were witnessed, a series of kinetic runs were completed. Fig. 7a–c shows the influence of varying temperature, catalyst load and the initial molar ratio of the reactants, respectively. As can be seen, the three variables show a positive effect on the kinetics of the reaction since the equilibrium position is reached more rapidly, as expected. Furthermore, Fig. 7c shows the marked effect of  $M$  on the maximum yield to solketal, which is enhanced by a variation from 3 to 12 from 34% to approximately 96%. This in turn evidences a significant shift of the ketalization reaction to the products. This observation agrees well with what was discussed in Section 1 regarding the large excess of acetone used for this reaction.

### 3.5. Kinetic modelling

Upon completion of 16 kinetic runs combining the variation of  $T$ ,  $M$  and catalyst load at various levels, enough data were obtained so as to propose and fit different kinetic models.

Considering the stoichiometry of the reaction and the virtually complete selectivity towards solketal as appointed in the Section 1, this is a simple reaction whose rate is equal to the rate of generation of the products as well as that of the consumption of reactants. Furthermore, owing to the equilibrium position discussed in the previous section, the reverse reaction from the products the reactant species needs to be taken into account.

Table 3 summarises all the kinetic models divided into three groups on which they are based, namely: potential laws (PL), Eley–Rideal (ER) and Langmuir–Hinshelwood–Hougen–Watson (LHHW). The base cases consider the dependence of the direct reaction with respect to the concentration of glycerol and acetone to a power of 1 and are designated by 1 in the three models. Models denoted as 2 and 3 are of zero order with respect to acetone and first order to glycerol and vice versa, respectively. Finally, models labelled as 4 account for zero order for both reactants. For all the models the reverse reaction was considered of first order with respect to solketal and water.

ER models are based on the assumption that only one of the molecules adsorbs onto the solid, while the other reacts with it directly from the fluid phase, without adsorbing. LHHW mechanisms, on the other hand, suggest that the two molecules adsorb and a bimolecular reaction takes place on the adjacent sites. Both mechanisms have been used to describe chemical reactions in sul-

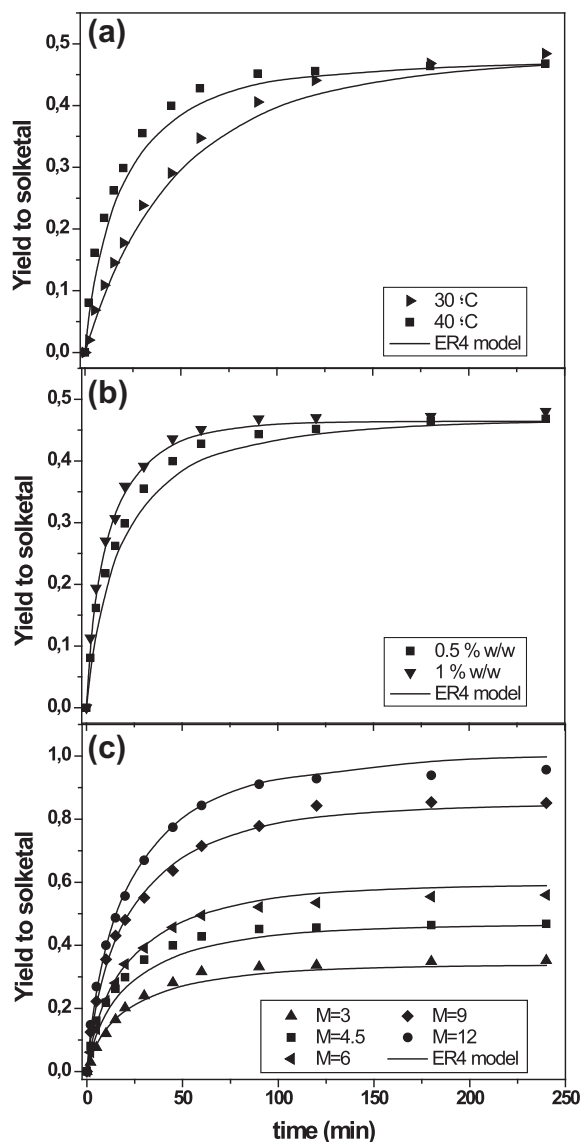


**Fig. 7.** Influence of (a) temperature, (b) catalyst load and (c) *M* on the evolution of the yield to Sk. Conditions: (a) *M* = 4.5 and catalyst load 0.5% w/w; (b) *T* = 40 °C and *M* = 4.5 and (c) *T* = 40 °C and catalyst load 0.5% w/w. Common conditions:  $\omega = 750$  rpm and  $d_p = 190$   $\mu\text{m}$ .

phonic resins: ER for Amberlyst 15 and Relite CFS in the esterification of fatty acids [55] or other resins for the synthesis of dimethyl ether [56] and LHHW for Amberlyst 15 in the dimerisation and trimerisation of methylbutenes [57]. PL models are pseudohomogeneous models that would consider virtually no adsorption of the species on the ion exchange resins. Thus, the reaction would take place solely in the fluid phase. In these models, the adsorption terms can be considered much lower than 1 in the denominator of the ER and LHHW models.

In the ER and LHHW models presented in Table 3, only the adsorption constant of W is included. More generalised models featuring the corresponding adsorption terms for the rest of the compounds involved were tried; nevertheless, fitting of such models to experimental data failed to converge. Suggestion of kinetic models neglecting adsorption terms other than that of water in the denominator of ER and LHHW models have previously been reported [36,58]. In sulphonic ion exchange resins the adsorption constant for water is generally very high compared to that of other components. For instance, in methyl acetate esterification catalysed by Amberlyst 15, a value of about four orders of magnitude higher than that of acetic acid was reported [59].

Additionally, the dependence of the kinetic constants  $k_1$  and  $k_2$  for the direct and reverse reactions with respect to temperature as well as the adsorption constant of water are given by the Arrhenius-based Eqs. (3) and (4):

$$\ln k_i = \ln k_{i0} - \frac{E_{ai}}{R} \cdot \frac{1}{T} \tag{3}$$

$$\ln K_w = \ln K_{w0} - \frac{\Delta H_{aw}}{R} \cdot \frac{1}{T} \tag{4}$$

where  $k_{i0}$  and  $E_{ai}/R$  are the preexponential factor of the kinetic constants and the ratio between activation energy and the ideal gas constant and  $\Delta H_{aw}/R$  is the ratio of the adsorption heat of water and the ideal gas constant.

As can be seen in Table 4, the degree of concordance between the experimental data and the predicted values together with the quality of the estimation of the model parameters, a relevant contrast exists among the models proffered.

For starters, bearing in mind the values retrieved for the models ER1, ER2, LHHW1 and LHHW2 can automatically be discarded: model ER1 gives an error in the estimation of the parameters of approximately one order of magnitude, whereas for the other three models the error amounts to various orders of magnitude. On the other hand, the rest of the models retrieved errors around one order of magnitude less than the mean value of the parameter. Consideration of models PL3, ER3 and LHHW3 enhances notably the degree of fitting with respect to models labelled 1 and 2. Even more significantly, models PL4, ER4 and LHHW4, of zero order with respect to both reactants, show a more accurate prediction according to the statistical criteria displayed in Table 4. This in turn accounts for the concentration of acetone and glycerol in the fluid phase being much lower than that in the solid phase, and the latter being practically constant at all times. This makes sense considering that the reaction is being performed in a solventless medium, where the concentrations of acetone and glycerol are high in the fluid medium. The two reacting species enter little by little into the resin competing for the active sites with the water molecules, whose affinity for sulphonic groups is much higher and thus cover most of the sulphonic groups. Additionally, following the statistical criteria defined in Section 2.3, it becomes clear that models labelled as 4 demonstrate a much better degree of fitting regardless of whether it is based on a PL, ER or LHHW equation rate.

**Table 3**  
Definition and nomenclature of the kinetic models proposed to correlate to experimental data.

Model name	Rate equation	Model name	Rate equation	Model name	Rate equation
PL1	$r = k_1 \cdot C_{cat} \cdot C_{Cly} \cdot C_{Ac} - k_2 \cdot C_{cat} \cdot C_{Sk} \cdot C_w$	ER1	$r = \frac{k_1 \cdot C_{cat} \cdot C_{Cly} \cdot C_{Ac} - k_2 \cdot C_{cat} \cdot C_{Sk} \cdot C_w}{1 + K_w \cdot C_w}$	LHHW1	$r = \frac{k_1 \cdot C_{cat} \cdot C_{Cly} \cdot C_{Ac} - k_2 \cdot C_{cat} \cdot C_{Sk} \cdot C_w}{(1 + K_w \cdot C_w)^2}$
PL2	$r = k_1 \cdot C_{cat} \cdot C_{Cly} - k_2 \cdot C_{cat} \cdot C_{Sk} \cdot C_w$	ER2	$r = \frac{k_1 \cdot C_{cat} \cdot C_{Cly} - k_2 \cdot C_{cat} \cdot C_{Sk} \cdot C_w}{1 + K_w \cdot C_w}$	LHHW2	$r = \frac{k_1 \cdot C_{cat} \cdot C_{Cly} - k_2 \cdot C_{cat} \cdot C_{Sk} \cdot C_w}{(1 + K_w \cdot C_w)^2}$
PL3	$r = k_1 \cdot C_{cat} \cdot C_{Ac} - k_2 \cdot C_{cat} \cdot C_{Sk} \cdot C_w$	ER3	$r = \frac{k_1 \cdot C_{cat} \cdot C_{Ac} - k_2 \cdot C_{cat} \cdot C_{Sk} \cdot C_w}{1 + K_w \cdot C_w}$	LHHW3	$r = \frac{k_1 \cdot C_{cat} \cdot C_{Ac} - k_2 \cdot C_{cat} \cdot C_{Sk} \cdot C_w}{(1 + K_w \cdot C_w)^2}$
PL4	$r = k_1 \cdot C_{cat} - k_2 \cdot C_{cat} \cdot C_{Sk} \cdot C_w$	ER4	$r = \frac{k_1 \cdot C_{cat} - k_2 \cdot C_{cat} \cdot C_{Sk} \cdot C_w}{1 + K_w \cdot C_w}$	LHHW4	$r = \frac{k_1 \cdot C_{cat} - k_2 \cdot C_{cat} \cdot C_{Sk} \cdot C_w}{(1 + K_w \cdot C_w)^2}$

**Table 4**  
Statistical comparison among the proposed kinetic models and values of the parameters retrieved with each model.

Model	Parameter	Value ± error	F	AIC	BIC	RMSE	VE (%)	Model	Parameter	Value ± error	F	AIC	BIC	RMSE	VE (%)
PL1	$\ln k_{10}$	14.29 ± 4.01	1.62·10 <sup>5</sup>	−2650	−3.15	0.204	91.08	ER4	$\ln k_{10}$	44.14 ± 5.12	2.12·10 <sup>6</sup>	−5149	−6.14	0.045	99.56
	$E_{a1}/R$ (K)	6879 ± 1234							$E_{a1}/R$ (K)	14920 ± 1558					
	$\ln k_{20}$	18.51 ± 7.28							$\ln k_{20}$	45.14 ± 4.97					
PL2	$E_{a2}/R$ (K)	7534 ± 2249	1.24·10 <sup>5</sup>	−2441	−2.90	0.231	88.53	LHHW1	$E_{a2}/R$ (K)	15318 ± 1513	1.76·10 <sup>5</sup>	−3099	−3.43	0.157	96.64
	$\ln k_{10}$	16.71 ± 4.58							$\ln K_{w0}$	51.17 ± 8.42					
	$E_{a1}/R$ (K)	6883 ± 1408							$\Delta H_{aw}/R$ (K)	15398 ± 2583					
PL3	$\ln k_{20}$	18.02 ± 7.94	9.33·10 <sup>5</sup>	−4123	−4.92	0.084	98.48	LHHW2	$\ln k_{10}$	527.84 ± 9.11·10 <sup>4</sup>	1.49·10 <sup>5</sup>	−2935	−3.21	0.171	93.66
	$E_{a2}/R$ (K)	7336 ± 2450							$E_{a1}/R$ (K)	1.62·10 <sup>5</sup> ± 2.76·10 <sup>7</sup>					
	$\ln k_{10}$	14.44 ± 1.39							$E_{a2}/R$ (K)	2.92·10 <sup>5</sup> ± 1.15·10 <sup>11</sup>					
PL4	$E_{a1}/R$ (K)	6775 ± 427	1.36·10 <sup>6</sup>	−4435	−5.30	0.070	98.60	LHHW3	$\ln K_{w0}$	272.34 ± 4.56·10 <sup>4</sup>	1.7·10 <sup>5</sup>	−4457	−5.45	0.064	99.12
	$\ln k_{20}$	18.55 ± 2.04							$\Delta H_{aw}/R$ (K)	8.21·10 <sup>5</sup> ± 1.38·10 <sup>7</sup>					
	$E_{a2}/R$ (K)	7373 ± 628							$\ln k_{10}$	886.55 ± 1.88·10 <sup>6</sup>					
ER1	$\ln k_{10}$	16.81 ± 1.13	1.42·10 <sup>5</sup>	−2892	−3.43	0.176	93.33	LHHW4	$E_{a1}/R$ (K)	269931 ± 1.27·10 <sup>21</sup>	2.10·10 <sup>6</sup>	−5143	−6.14	0.046	99.55
	$E_{a1}/R$ (K)	6753 ± 346							$\ln k_{20}$	68.79 ± 4.19·10 <sup>18</sup>					
	$\ln k_{20}$	18.45 ± 1.62							$E_{a2}/R$ (K)	30400 ± 1.27·10 <sup>21</sup>					
ER2	$E_{a2}/R$ (K)	7321 ± 501	1.13·10 <sup>5</sup>	−2707	−3.21	0.197	91.67	LHHW4	$\ln K_{w0}$	448.03 ± 9.38·10 <sup>5</sup>	2.10·10 <sup>6</sup>	−5143	−6.14	0.046	99.55
	$\ln k_{10}$	65.50 ± 512.51							$\Delta H_{aw}/R$ (K)	135.302 ± 2.84·10 <sup>8</sup>					
	$E_{a1}/R$ (K)	21,579 ± 155,512							$\ln k_{10}$	34.21 ± 4.44					
ER3	$\ln k_{20}$	89.28 ± 509.72	1.06·10 <sup>5</sup>	−4576	−5.45	0.064	99.15	LHHW4	$E_{a1}/R$ (K)	12,660 ± 1356	2.10·10 <sup>6</sup>	−5143	−6.14	0.046	99.55
	$E_{a2}/R$ (K)	28,484 ± 154,646							$\ln k_{20}$	37.23 ± 4.44					
	$\ln K_{w0}$	51.91 ± 519.79							$E_{a2}/R$ (K)	12,953 ± 1281					
ER4	$\Delta H_{aw}/R$ (K)	14,572 ± 157,736	1.13·10 <sup>5</sup>	−2707	−3.21	0.197	91.67	LHHW4	$\ln K_{w0}$	34.11 ± 7.76	2.10·10 <sup>6</sup>	−5143	−6.14	0.046	99.55
	$\ln k_{10}$	71.65 ± 4.78·10 <sup>6</sup>							$\Delta H_{aw}/R$ (K)	10,517 ± 2402					
	$E_{a1}/R$ (K)	19,824 ± 1.45·10 <sup>9</sup>							$\ln k_{10}$	35.20 ± 2.84					
ER5	$\ln k_{20}$	93.21 ± 4.78·10 <sup>6</sup>	1.06·10 <sup>5</sup>	−4576	−5.45	0.064	99.15	LHHW4	$E_{a1}/R$ (K)	12,222 ± 869	2.10·10 <sup>6</sup>	−5143	−6.14	0.046	99.55
	$E_{a2}/R$ (K)	26,743 ± 1.45·10 <sup>9</sup>							$\ln k_{20}$	35.96 ± 2.69					
	$\ln K_{w0}$	53.70 ± 4.78·10 <sup>6</sup>							$E_{a2}/R$ (K)	12,547 ± 822					
ER6	$\Delta H_{aw}/R$ (K)	12,186 ± 1.45·10 <sup>9</sup>	1.06·10 <sup>5</sup>	−4576	−5.45	0.064	99.15	LHHW4	$\ln K_{w0}$	32.59 ± 5.16	2.10·10 <sup>6</sup>	−5143	−6.14	0.046	99.55
	$\ln k_{10}$	43.72 ± 8.33							$\Delta H_{aw}/R$ (K)	10,058 ± 1597					
	$E_{a1}/R$ (K)	15,530 ± 2535													
ER7	$\ln k_{20}$	47.04 ± 8.10	1.06·10 <sup>5</sup>	−4576	−5.45	0.064	99.15	LHHW4			2.10·10 <sup>6</sup>	−5143	−6.14	0.046	99.55
	$E_{a2}/R$ (K)	15,913 ± 2463													
	$\ln K_{w0}$	53.88 ± 13.25													
ER8	$\Delta H_{aw}/R$ (K)	16,221 ± 4063	1.06·10 <sup>5</sup>	−4576	−5.45	0.064	99.15	LHHW4			2.10·10 <sup>6</sup>	−5143	−6.14	0.046	99.55

Statistical comparison among PL4, ER4 and LHHW4 lead to dismiss PL4. However, ER4 and LHHW4 show very similar goodness of fit, with the former performing slightly better in statistical terms. Though a LHHW model has been reported previously for this reaction [36] and represents with adequacy our data, an ER model appears more plausible. The LHHW model would involve the adsorption of glycerol onto an adjacent active site to another onto which a molecule of acetone is already adsorbed. This, in principle is much less likely to happen considering that the affinity of sulphonic groups for alcohols or glycerol would be lower due to the structure of the molecule compared to acetone. In addition, molar excess of acetone with respect to glycerol was used ranging from 3 to 12, lowering the likelihood of glycerol adsorbing right next to acetone.

The values of  $E_{a1}/R$  and  $E_{a2}/R$  retrieved from correlation give values of the activation energies of the direct and reverse reaction equal to  $124.0 \pm 12.9$  kJ/mol and  $127.3 \pm 12.6$  kJ/mol. These values concur with the chemical reaction being the controlling step, for activation energies are usually within the range from 40 to 200 kJ/mol for chemical reaction-controlled processes. The heat of adsorption of water deduced was  $128.0 \pm 21.4$  kJ/mol, which is approximately twice as much as those reported on an Amberlyst 35 resin for the solvent-assisted ketalization of glycerol, 64.7 kJ/mol [36], or an Amberlyst 15 for the esterification of nonanoic acid with methanol, 60.7 kJ/mol [60].

For all of these reasons, ER4 is selected as the model that best explains the kinetics of the reaction. Finally, Fig. 8 demonstrates that the model chosen is capable of predicting the vast majority of the experimental data within a margin of error of 10%.

Although ketalization of glycerol and acetone is known to be a reversible reacting system, deactivation of sulphonic acids is also well-known, mainly in esterification processes, due to a variety

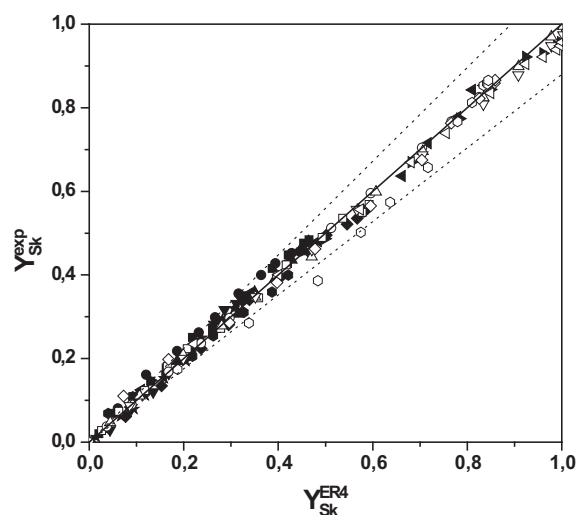


**Fig. 8.** Validation of the LHHW4 model with all the experimental data available.

of mechanisms: active phase hydration, cation exchange, and catalytic site blockage [32,61]. The use of pure reagents reduces or avoids to a certain extension the deactivation of the catalysts in one or several runs when obtaining solketal from glycerol [32]. It is more common to observe this phenomenon when working in esterification reactions or when using bio-glycerol from the biodiesel production process [32,62,63]. When deactivation takes place, the inclusion of equations in the kinetic model is needed to obtain the better values for goodness-of-fit parameters (RMSE, VE, F-value, AIC) [62]. There are excellent values for VE, higher than 99%, and very low values of RMSE, with very high values for F, in

the case of the chosen kinetic model. Thus, little improvement could be obtained by including deactivation as an additional phenomenon when working in batch conditions and low reaction time values, but cation exchange could result in catalyst deactivation if using continuous operation without regeneration and technical- or lower grade glycerol. Regeneration of sulphonic acid resins by using cation exchange with strong acids is relatively simple and restores most of its activity, if not all, depending on the presence or absence of cations and organic impurities in the reacting system [64].

#### 4. Conclusions

The solventless synthesis of solketal has been successfully completed in batch operation making use of the sulphonic ion exchange resin Lewatit GF101. A liquid–liquid–solid system is dealt with herein, in which the study of the external and internal mass transfer becomes significant, leading to the conclusion that using an agitation speed of 750 rpm the former is negligible and that a particle size of 190  $\mu\text{m}$  is sufficient so as to ignore the latter. A series of kinetic runs were performed varying temperature, molar excess of acetone to glycerol and amount of catalyst, observing that the three variables had a positive effect in kinetic terms and that the effect of the molar excess of acetone on the equilibrium is very significant. A series of kinetic models were proposed based on potential laws to account for pseudohomogeneous models as well as Eley–Rideal and Langmuir–Hinshelwood–Hougen–Watson rate equations. After considering the plausible reaction mechanism and accounting for physical and statistical criteria, an ER model was selected. This model featured the following considerations: reverse reaction from the products, zero order with respect to the reactant species and no adsorption terms for any species other than water in the denominator. From multivariable fitting, the activation energies for the direct and reverse reaction and the adsorption constant of water were  $124.0 \pm 12.9$  kJ/mol,  $127.3 \pm 12.6$  kJ/mol and  $128.0 \pm 21.4$  kJ/mol, respectively.

#### Acknowledgments

The authors would like to thank the labour of the NMR Research Associated Centre at the College of Chemical Sciences at the Complutense University of Madrid. Additionally, grateful appreciation goes to the Ministry of Science and Innovation (projects CTQ2007-60919 and CTQ2010-15460) for financial support.

#### Appendix A. Supplementary data

Supplementary data associated with this article can be found, in the online version, at <http://dx.doi.org/10.1016/j.cej.2015.01.107>.

#### References

- [1] A. Behr, J. Eilting, K. Irawadi, J. Leschinski, F. Lindner, Improved utilisation of renewable resources: new important derivatives of glycerol, *Green Chem.* 10 (2008) 13–30.
- [2] A. Behr, J.P. Gomes, The refinement of renewable resources: new important derivatives of fatty acids and glycerol, *Eur. J. Lipid Sci. Technol.* 112 (2010) 31–50.
- [3] M. Pagliaro, M. Rossi, *The Future of Glycerol: New Uses of a Versatile Raw Material*, RSC Publishing, Cambridge, UK, 2008.
- [4] C.-H. Zhou, J.N. Beltrami, Y.-X. Fan, G.Q. Lu, Chemoselective catalytic conversion of glycerol as a biorenewable source to valuable commodity chemicals, *Chem. Soc. Rev.* 37 (2008) 527–549.
- [5] J. Kenar, Glycerol as a platform chemical: sweet opportunities on the horizon?, *Lipid Technol.* 19 (2007) 249–253.
- [6] M. Pagliaro, R. Ciriminna, H. Kimura, M. Rossi, C. Della, Pina, Recent advances in the conversion of bioglycerol into value-added products, *Eur. J. Lipid Sci. Technol.* 111 (2009) 788–799.
- [7] J.A. Melero, G. Vicente, G. Morales, M. Paniagua, J.M. Moreno, R. Roldan, A. Ezquerro, C. Perez, Acid-catalyzed etherification of bio-glycerol and isobutylene over sulfonic mesostructured silicas, *Appl. Catal. A* 346 (2008) 44–51.
- [8] K. Klepáčová, D. Mravec, A. Kaszonyi, M. Bajus, Etherification of glycerol and ethylene glycol by isobutylene, *Appl. Catal. A* 328 (2007) 1–13.
- [9] R. Wessendorf, Glycerol derivatives as fuel components, *Erdöl & Kohle Erdgas Petrochemie* 48 (1995) 138–143.
- [10] H. Noureddini, Production of oxygenated biodiesel fuel of low cloud point, US6015440-A.
- [11] F.J. Liotta, H.S. Kesling, L.J. Karas, Transesterifying fat with alcohol and iron oxide or alumina catalyst[comprises diesel fuel hydrocarbon(s) and particulate emission reducing amt. of di- or tri-alkyl glycerol ether, US5308365-A.
- [12] R.S. Karinen, A.O.I. Krause, New biocomponents from glycerol, *Appl. Catal. A* 306 (2006) 128–133.
- [13] J.A. Melero, R. van Grieken, G. Morales, M. Paniagua, Acidic mesoporous silica for the acetylation of glycerol: synthesis of bioadditives to petrol fuel, *Energy Fuels* 21 (2007) 1782–1791.
- [14] N. Rahmat, A.Z. Abdullah, A.R. Mohamed, Recent progress on innovative and potential technologies for glycerol transformation into fuel additives: a critical review, *Renew. Sustain. Energy Rev.* 14 (2010) 987–1000.
- [15] A.L. Maksimov, A.I. Nekhaev, D.N. Ramazanov, Y.A. Arinicheva, A.A. Dzyubenko, S.N. Khadzhev, Preparation of high-octane oxygenate fuel components from plant-derived polyols, *Pet. Chem.* 51 (2011) 61–69.
- [16] C.J.A. Mota, C.X.A. da Silva, N. Rosenbach Jr., J. Costa, F. da Silva, Glycerin derivatives as fuel additives: the addition of glycerol/acetone ketal (solketal) in gasolines, *Energy Fuels* 24 (2010) 2733–2736.
- [17] E. Garcia, M. Laca, E. Perez, A. Garrido, J. Peinado, New class of acetal derived from glycerin as a biodiesel fuel component, *Energy Fuels* 22 (2008) 4274–4280.
- [18] N. Suriyaprapadilok, B. Kitiyanan, Synthesis of solketal from glycerol and its reaction with benzyl alcohol, in: 9th Eco-Energy and Materials Science and Engineering Symposium, 2011.
- [19] M. Selva, V. Benedet, M. Fabris, Selective catalytic etherification of glycerol formal and solketal with dialkyl carbonates and  $\text{K}_2\text{CO}_3$ , *Green Chem.* 14 (2012) 188–200.
- [20] S. Budavari, *Merck Index*, eleventh ed., Merck & Co. Inc., Rahway, New Jersey, 1989.
- [21] J. Jurczak, S. Pikul, T. Bauer, *Tetrahedron* 42 (1986) 447–488.
- [22] R.P. Hof, R.M. Kellogg, Synthesis and lipase-catalyzed resolution of 5-(hydroxymethyl)-1,3-dioxolan-4-ones: masked glycerol analogs as potential building blocks for pharmaceuticals, *J. Org. Chem.* 61 (1996) 3423–3427.
- [23] V. Calvino-Casilda, K. Stawicka, M. Trejda, M. Ziolek, M.A. Banares, Real-time Raman monitoring and control of the catalytic acetalization of glycerol with acetone over modified mesoporous cellular foams, *J. Phys. Chem. C* 118 (2014) 10780–10791.
- [24] M.S. Khayoon, B.H. Hameed, Solventless acetalization of glycerol with acetone to fuel oxygenates over Ni–Zr supported on mesoporous activated carbon catalyst, *Appl. Catal. A* 464 (2013) 191–199.
- [25] N. Suriyaprapadilok, B. Kitiyanan, Synthesis of solketal from glycerol and its reaction with benzyl alcohol, *Energy Procedia* 9 (2011) 63–69.
- [26] B. Bruchmann, K. Haerberle, H. Gruner, M. Hirn, Preparation of cyclic acetals or ketals, especially isopropylidene glycerin[comprising distilling off some of aldehyde or ketone during reaction with polyol, 1999, EP842929-A.
- [27] F.D.L. Menezes, M.D.O. Guimaraes, M.J. da Silva, Highly selective  $\text{SnCl}_2$ -catalyzed solketal synthesis at room temperature, *Ind. Eng. Chem. Res.* 52 (2013) 16709–16713.
- [28] H. Matsushita, M. Shibagaki, K. Takahashi, H. Kuno, Method of preparing acetal or ketal, 1989, US Patent 4,841,075.
- [29] J. Deutsch, A. Martin, H. Lieske, Investigations on heterogeneously catalysed condensations of glycerol to cyclic acetals, *J. Catal.* 245 (2007) 428–435.
- [30] J.S. Clarkson, A.J. Walker, M.A. Wood, Continuous reactor technology for ketal formation: an improved synthesis of solketal, *Org. Process Res. Dev.* 5 (2001) 630–635.
- [31] P. Ferreira, I.M. Fonseca, A.M. Ramos, J. Vital, J.E. Castanheiro, Valorisation of glycerol by condensation with acetone over silica-included heteropolyacids, *Appl. Catal. B* 98 (2010) 94–99.
- [32] G. Vicente, J.A. Melero, G. Morales, M. Paniagua, E. Martin, Acetalisation of bio-glycerol with acetone to produce solketal over sulfonic mesostructured silicas, *Green Chem.* 12 (2010) 899–907.
- [33] L. Li, T.I. Koranyi, B.F. Sels, P.P. Pescarmona, Highly-efficient conversion of glycerol to solketal over heterogeneous Lewis acid catalysts, *Green Chem.* 14 (2012) 1611–1619.
- [34] P.S. Reddy, P. Sudarsanam, B. Malleshm, G. Raju, B.M. Reddy, Acetalisation of glycerol with acetone over zirconia and promoted zirconia catalysts under mild reaction conditions, *J. Ind. Eng. Chem.* 17 (2011) 377–381.
- [35] D. Nandan, P. Sreenivasulu, L.N.S. Konathala, M. Kumar, N. Viswanadham, Acid functionalized carbon-silica composite and its application for solketal production, *Microporous Mesoporous Mater.* 179 (2013) 182–190.
- [36] M.R. Nanda, Z. Yuan, W. Qin, H.S. Ghaziaskar, M.-A. Poirier, C.C. Xu, Thermodynamic and kinetic studies of a catalytic process to convert glycerol into solketal as an oxygenated fuel additive, *Fuel* 117 (2014) 470–477.
- [37] M.R. Nanda, Z. Yuan, W. Qin, H.S. Ghaziaskar, M.-A. Poirier, C. Xu, A new continuous-flow process for catalytic conversion of glycerol to oxygenated fuel additive: catalyst screening, *Appl. Energy* 123 (2014) 75–81.

- [38] C.X.A. da Silva, V.L.C. Goncalves, C.J.A. Mota, Water-tolerant zeolite catalyst for the acetalisation of glycerol, *Green Chem.* 11 (2009) 38–41.
- [39] C.X.A. da Silva, C.J.A. Mota, The influence of impurities on the acid-catalyzed reaction of glycerol with acetone, *Biomass Bioenergy* 35 (2011) 3547–3551.
- [40] B. Bruchmann, K. Haberle, H. Gruner, M. Hirn, Preparation of cyclic acetals or ketals, 1999, US Patent 5,917,059.
- [41] D. Royon, S. Locatelli, E.E. Gonzo, Ketalization of glycerol to solketal in supercritical acetone, *J. Supercrit. Fluids* 58 (2011) 88–92.
- [42] L. Roldan, R. Mallada, J.M. Fraile, J.A. Mayoral, M. Menendez, Glycerol upgrading by ketalization in a zeolite membrane reactor, *Asia-Pac. J. Chem. Eng.* 4 (2009) 279–284.
- [43] M.R. Nanda, Z. Yuan, W. Qin, H.S. Ghaziaskar, M.-A. Poirier, C. Xu, Catalytic conversion of glycerol to oxygenated fuel additive in a continuous flow reactor: process optimization, *Fuel* 128 (2014) 113–119.
- [44] J. Esteban, A.J. Vorholt, A. Behr, M. Ladero, F. Garcia-Ochoa, Liquid–liquid equilibria for the system acetone + solketal + glycerol at 303.2, 313.2 and 323.2 K, *J. Chem. Eng. Data* 59 (2014) 2850–2855.
- [45] J.J. Tamayo, M. Ladero, V.E. Santos, F. Garcia-Ochoa, Esterification of benzoic acid and glycerol to  $\alpha$ -monobenzoate glycerol in solventless media using an industrial free *Candida antarctica* lipase B, *Process Biochem.* 47 (2012) 243–250.
- [46] M. Ladero, M. de Gracia, F. Trujillo, F. Garcia-Ochoa, Phenomenological kinetic modelling of the esterification of rosin and polyols, *Chem. Eng. J.* 197 (2012) 387–397.
- [47] L. Zhou, T.-H. Nguyen, A.A. Adesina, The acetylation of glycerol over amberlyst-15: kinetic and product distribution, *Fuel Process. Technol.* 104 (2012) 310–318.
- [48] R. Xu, Measuring explained variation in linear mixed effects models, *Stat. Med.* 22 (2003) 3527–3541.
- [49] H. Akaike, A new look at the statistical model identification, *IEEE Trans. Autom. Control* 19 (1974) 716–723.
- [50] J. Esteban, E. Fuente, A. Blanco, M. Ladero, F. Garcia-Ochoa, Phenomenological kinetic model of the synthesis of glycerol carbonate assisted by focused beam reflectance measurements, *Chem. Eng. J.* 260 (2015) 434–443.
- [51] F. Garcia-Ochoa, A. Romero, J. Querol, Modeling of the thermal normal-octane oxidation in the liquid phase, *Ind. Eng. Chem. Res.* 28 (1989) 43–48.
- [52] H. Topallar, Y. Bayrak, The effect of temperature on the dynamic viscosity of acetone sunflower-seed oil mixtures, *Turk. J. Chem.* 22 (1998) 361–366.
- [53] J.B. Segur, H.E. Oberstar, Viscosity of glycerol and its aqueous solutions, *Ind. Eng. Chem.* 43 (1951) 2117–2120.
- [54] A.E. Hoerl, Fitting curves to data, in: J.H. Perry (Ed.), *Chemical Business Handbook*, McGraw-Hill, New York, 1954, pp. 55–57.
- [55] R. Tesser, L. Casale, D. Verde, M. Di Serio, E. Santacesaria, Kinetics and modeling of fatty acids esterification on acid exchange resins, *Chem. Eng. J.* 157 (2010) 539–550.
- [56] Z. Lei, Z. Zou, C. Dai, Q. Li, B. Chen, Synthesis of dimethyl ether (DME) by catalytic distillation, *Chem. Eng. Sci.* 66 (2011) 3195–3203.
- [57] M. Granollers, J.F. Izquierdo, C. Fite, F. Cunill, Kinetic study of methyl-butenes dimerization and trimerization in liquid-phase over a macroporous acid resin, *Chem. Eng. J.* 234 (2013) 266–275.
- [58] J. Lilja, D.Y. Murzin, T. Salmi, J. Aumo, P.M. Arvela, M. Sundell, Esterification of different acids over heterogeneous and homogeneous catalysts and correlation with the Taft equation, *J. Mol. Catal. A: Chem.* 182 (2002) 555–563.
- [59] W.F. Yu, K. Hidajat, A.K. Ray, Determination of adsorption and kinetic parameters for methyl acetate esterification and hydrolysis reaction catalyzed by Amberlyst 15, *Appl. Catal. A* 260 (2004) 191–205.
- [60] M. Sharma, R.K. Wanchoo, A.P. Toor, Adsorption and kinetic parameters for synthesis of methyl nonanoate over heterogeneous catalysts, *Ind. Eng. Chem. Res.* 51 (2012) 14367–14375.
- [61] J.A. Melero, L. Fernando Bautista, J. Iglesias, G. Morales, R. Sanchez-Vazquez, K. Wilson, A.F. Lee, New insights in the deactivation of sulfonic modified SBA-15 catalysts for biodiesel production from low-grade oleaginous feedstock, *Appl. Catal. A* 488 (2014) 111–118.
- [62] L. Molinero, M. Ladero, J.J. Tamayo, F. Garcia-Ochoa, Homogeneous catalytic esterification of glycerol with cinnamic and methoxycinnamic acids to cinnamate glycerides in solventless medium: kinetic modeling, *Chem. Eng. J.* 247 (2014) 174–182.
- [63] M.R. Nanda, Z. Yuan, W. Qin, H.S. Ghaziaskar, M.A. Poirier, C. Xu, A new continuous-flow process for catalytic conversion of glycerol to oxygenated fuel additive: catalyst screening, *Appl. Energy* 123 (2014) 75–81.
- [64] X. Hu, C. Lievens, D. Mourant, Y. Wang, L. Wu, R. Gunawan, Y. Song, C.-Z. Li, Investigation of deactivation mechanisms of a solid acid catalyst during esterification of the bio-oils from mallee biomass, *Appl. Energy* 111 (2013) 94–103.